

UC Davis

UC Davis Previously Published Works

Title

Gain-of-function of the 1-aminocyclopropane-1-carboxylate synthase gene ACS1G induces female flower development in cucumber gynoecey

Permalink

<https://escholarship.org/uc/item/6k82j2f2>

Journal

The Plant Cell, 33(2)

ISSN

1040-4651

Authors

Zhang, Huimin
Li, Shuai
Yang, Li
et al.

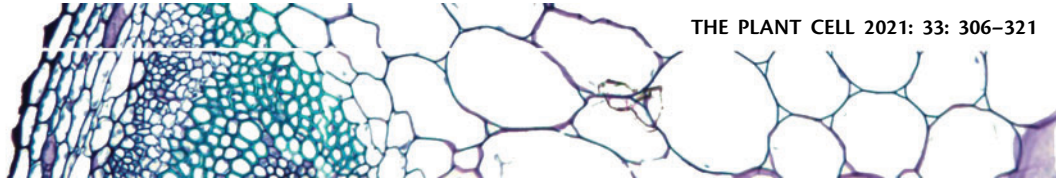
Publication Date

2021-04-17


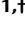














DOI

10.1093/plcell/koaa018

Peer reviewed



Gain-of-function of the 1-aminocyclopropane-1-carboxylate synthase gene *ACS1G* induces female flower development in cucumber gynoecy

Huimin Zhang ^{1,2,†}, Shuai Li ^{1,†}, Li Yang ^{2,3,†}, Guanghua Cai ^{2,†}, Huiming Chen ⁴, Dongli Gao ², Tao Lin ², Qingzhi Cui ⁴, Donghui Wang ⁵, Zheng Li ⁶, Run Cai ⁷, Shunong Bai ⁵, William J. Lucas ^{2,8}, Sanwen Huang ², Zhonghua Zhang ^{1,9,*}, and Jinjing Sun ^{1,*}

- 1 Institute of Vegetables and Flowers, Chinese Academy of Agricultural Sciences, Key Laboratory of Biology and Genetic Improvement of Horticultural Crops of the Ministry of Agriculture, Sino-Dutch Joint Laboratory of Horticultural Genomics, Beijing 100081, China
- 2 Genome Analysis Laboratory of the Ministry of Agriculture, Agricultural Genomics Institute at Shenzhen, Chinese Academy of Agricultural Sciences, Shenzhen 518124, China
- 3 College of Horticulture and Forestry, Huazhong Agricultural University and Key Laboratory of Horticultural Plant Biology, Ministry of Education, Wuhan 430070, China
- 4 Hunan Vegetable Research Institute, Hunan Academy of Agricultural Science, Changsha 410125, China
- 5 College of Life Sciences, Peking University, Beijing 100871, China
- 6 College of Horticulture, Northwest A&F University, Shaanxi 712100, China
- 7 School of Agriculture and Biology, Shanghai Jiao Tong University, Shanghai 200240, China
- 8 College of Biological Sciences, University of California, Davis, CA 95616, USA
- 9 College of Horticulture, Qingdao Agricultural University, Qingdao 266109, China

*Authors for correspondence: sunjjing@caas.cn, zhangzhonghua@caas.cn

†These authors contributed equally to this work.

The authors responsible for distribution of materials integral to the findings presented in this article in accordance with the policy described in the Instructions for Authors (www.plantcell.org) are: Jinjing Sun (sunjjing@caas.cn) and Zhonghua Zhang (zhangzhonghua@caas.cn).

S.H., Z.Z., J.S. and S.B. designed the project; J.S., H.Z., L.Y., S.L., H.C., G.C., D.G., Q.C. and D.W. performed the research; J.S., R.C., Z.L., T.L. and W.J.L. analyzed the data; J.S., H.Z., L.Y., and S.L. wrote the original draft article; W.J.L., S.B., S.H., J.S., and Z.Z. wrote the final article, which was approved by all authors.

Unisexual flowers provide a useful system for studying plant sex determination. In cucumber (*Cucumis sativus* L.), three major Mendelian loci control unisexual flower development, *Female* (*F*), *androecious* [*a*; 1-aminocyclopropane-1-carboxylate {*ACC*} synthase 11, *acs11*], and *Monoecious* (*M*; *ACS2*), referred to here as the Female, Androecious, Monoecious (FAM) model, in combination with two genes, *gynoecious* (*g*, the WIP family C2H2 zinc finger transcription factor gene *WIP1*) and the ethylene biosynthetic gene *ACC oxidase 2* (*ACO2*). The *F* locus, conferring gynoecy and the potential for increasing fruit yield, is defined by a 30.2-kb tandem duplication containing three genes. However, the gene that determines the *Female* phenotype, and its mechanism, remains unknown. Here, we created a set of mutants and revealed that *ACS1G* is responsible for gynoecy conferred by the *F* locus. The duplication resulted in *ACS1G* acquiring a new promoter and expression pattern; in plants carrying the *F* locus duplication, *ACS1G* is expressed early in floral bud development, where it functions with *ACO2* to generate an ethylene burst. The resulting ethylene represses *WIP1* and activates *ACS2* to initiate gynoecy. This early *ACS1G* expression bypasses the need for *ACS11* to produce ethylene, thereby establishing a dominant pathway for female floral development. Based on these findings, we propose a model for how these ethylene biosynthesis genes cooperate to control unisexual flower development in cucumber.

Introduction

Unisexual flower development represents a model experimental system to decipher the regulatory mechanism of sex determination in plants (Tanurdzic and Banks, 2004; Ma and Pannell, 2016). Considerable attention has been devoted to identifying genes that control male and female flower development (Banks, 2008; Aryal and Ming, 2014). Cucumber (*Cucumis sativus* L.) represents one such system (Malepszy and Niemirowiczszczytt, 1991; Ainsworth and Buchanan-Wollaston, 1997), and the female flower ratio is an important yield trait for cucumber as only female flowers develop economically valuable fruit.

A pioneering genetic study established that different cucumber lines exhibit stable unisexual flower distribution phenotypes (Galun, 1962). These phenotypes included plants that produce only female flowers (termed gynoecious), both male and female flowers (termed monoecious), only male flowers (termed androecious), only bisexual flowers (hermaphrodite), and male and bisexual flowers (termed andromonoecious) (Perl-Treves, 1999). Major genetic loci were identified, named *Female* (*F*), *androecious* (*a*), and *Monoecious* (*M*), which determine the distribution of unisexual flowers (Galun, 1962; Kubicki, 1969a; Kubicki, 1969b, 1969c). For convenience, we term this system the FAM model. Gynoecious cucumbers conferred by the *F* locus have been used, for almost half a century, specifically in breeding greenhouse varieties with high yield potential.

Early studies also identified ethylene as a key regulator in male and female flower development; for example, application of ethephon promotes female flower development (Wittwer and Hillyer, 1954; Iwahori et al., 1970; Byers et al., 1972). Although other phytohormones were examined for their effects on the ratio of unisexual flowers, ethylene was widely accepted as a key regulator of unisexual flower development in cucumber (Yin and Quinn, 1992).

During this same period, the ethylene biosynthetic pathway was deciphered, and this established that methionine is converted into *S*-adenosylmethionine (SAM) by methionine adenosyltransferase; SAM is then converted into 1-aminocyclopropane-1-carboxylate (ACC) by ACC synthase (ACS). Finally, ACC is oxidized to ethylene by ACC oxidase (ACO). Here, ACS and ACO function as key enzymes for ethylene production (Adams and Yang, 1979). Almost all major genes controlling flower sex type encode key enzymes involved in ethylene biosynthesis, with *WIP1*, which encodes a C2H2 zinc finger transcription factor of the WIP family, being the exception. The *M* gene encodes ACS2, another ACS expressed in the carpel region of the female flower; its inactivation (*m*) results in formation of a bisexual flower (Boualem et al., 2008; Li et al., 2009). The *A* gene encodes ACS11 and a dysfunctional ACS11 (*a* gene) blocks the female flower developmental pathway (Boualem et al., 2015).

The ACO2 was also shown to affect unisexual flower development, through its coordination with ACS11 in floral preferential production of ethylene; defective ACO2 results in the loss of female flowers (Chen et al., 2016). Finally,

WIP1 was identified as a C2H2 zinc finger transcription factor required for male flower development; its expression is repressed by ACS11 (Martin et al., 2009; Boualem et al., 2015; Hu et al., 2017). Without *WIP1* expression, or when *WIP1* is dysfunctional, cucumber plants produce female flowers, but with some bisexual flowers being formed at the lower (earlier) nodes (Hu et al., 2017).

Although many studies have clarified the roles of other loci, the mechanisms by which the *F* locus affects sex determination in cucumber remain unclear. The discovery that the *F* locus contains an additional copy of *ACS1* (diagrammed in Figure 1A) provided an initial link between ethylene production and female flower development (Trebitsh et al., 1997). However, although the *F* gene was suggested to encode gynoecious *Cucumis sativus* ACC synthase (ACS1G) (Mibus and Tatlioglu, 2004; Knopf and Trebitsh, 2006), genome-wide mapping of structural variation revealed that the *F* locus is a 30.2-kb tandem duplicated region. This region contains not only ACS1G but also other genes (Zhang et al., 2015) that, to date, have not been ruled out as participants in the *F* locus. Additionally, currently, there is no evidence to determine whether the female promotion function of the *F* locus represents a dosage effect of multiple copies of ACS1, or alternatively, a function conferred by ACS1G by acquiring a novel promoter through recombination.

An earlier study using RNA interference to downregulate ACS1 and ACS1G expressions, in the cucumber *FF* genotype, reported that this caused a transition from gynoecey to monoecy, which was offered as support for the hypothesis that ACS1G confers a simple dosage effect (Shiber et al., 2008). However, this result could not distinguish between the functions of ACS1 and ACS1G, as the entire untranslated and coding regions of ACS1 and ACS1G are identical, and the cucumber *FF* genotype contains both ACS1 and ACS1G. Thus, the genetic regulatory mechanism underlying the molecular basis of the *F* gene remains to be fully elucidated.

Another problem in deciphering the molecular mechanism underlying the genetic control over unisexual flower development is that, in the current FAM model, the criteria to define a unisexual flower are based on the entire flower; i.e., male or female flowers. However, unisexual flowers result from abnormal floral organ development (Dellaporta and Calderon-Urrea, 1993; Ainsworth and Buchanan-Wollaston, 1997). Although it was established that ethylene plays a key role in cucumber female flower development, little is known about whether ethylene is required for carpel development and/or inhibition of stamen development.

In this regard, it was demonstrated that primordial anther-specific DNA damage is closely correlated with stamen arrest in the female cucumber flower (Hao et al., 2003). Subsequently, it was shown that this anther-specific DNA damage was caused by the stamen preferential downregulation of the ethylene receptor (*ETR*) gene, *Cs-ETR1* (Wang et al., 2010), and such organ preferential downregulation of *Cs-ETR1* is caused by a B-class APETALA (AP)-type MADS (*MCM1*, *AG*, *DEF*, *SRF*)-box gene, *Cs-AP3* (Sun et al., 2016).

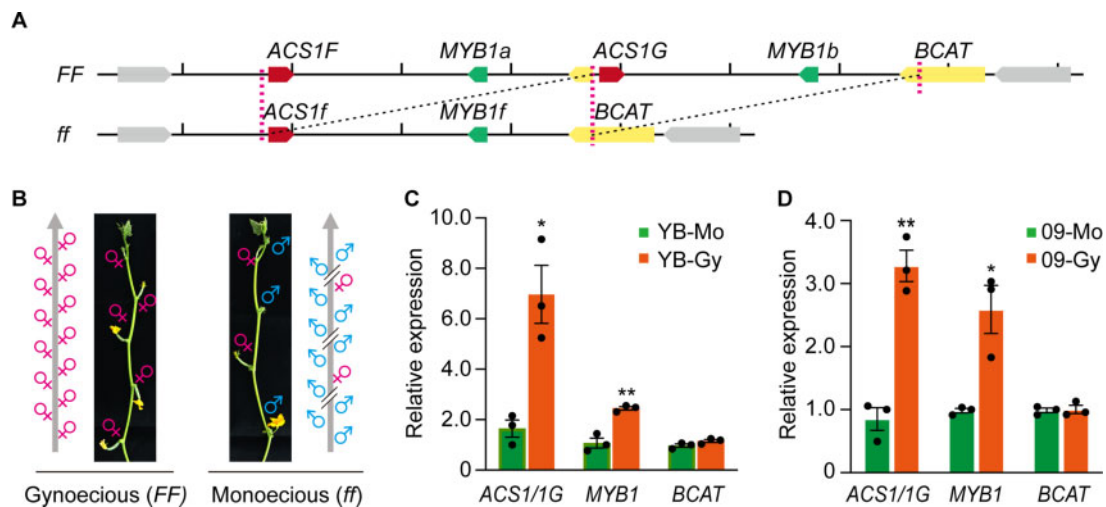


Figure 1 Genomic organization and gene expression pattern of the cucumber *F* locus. (A) Structural organization of the 30.2-kb duplicated region in gynoecious compared with monoecious cucumber lines. *ACS1F*, *ACS1f*, and *ACS1G*, *CsaV3_6G044400*; *MYB1a*, *MYB1b*, *MYB1f*, *CsaV3_6G044410*; *BCAT*, *CsaV3_6G044420*. The yellow box in front of *ACS1G*, in the *F* locus, represents part of *BCAT*. The magenta vertical dashed lines present the tandem duplication unit, of the *F* locus. (B) Representation of the phenotypes of *FF* and *ff* genotypes. The *FF* genotype is gynoecious, whereas the *ff* genotype is monoecious. (C and D) Relative expression levels of *ACS1/1G*, *MYB1*, and *BCAT* in gynoecious and monoecious near-isogenic lines. YB-Mo and O9-Mo are monoecious; YB-Gy and O9-Gy are gynoecious. YB-Mo and YB-Gy, and O9-Mo and O9-Gy, are isogenic lines, respectively. Data are presented as mean \pm SEM, $n = 3$. * $p < 0.05$ and ** $p < 0.01$ in Student's *t*-test compared to the isogenic monoecious lines (Supplemental Data Set 1). *BCAT*, Branched Chain Amino Acid Transaminase.

Finally, ethylene-induced expression of a calcium-dependent DNase gene, *Cs-CaN*, is correlated with the anther-specific DNA damage (Gu et al., 2011). Taken together, these findings support the hypothesis that ethylene plays a direct role in the inhibition of anther primordia development, in female cucumber flowers, through a stamen-specific ethylene perception and downstream response. However, a remaining question is why are ethylene synthesis genes playing key roles in promoting female flower development?

Based on current information, it would appear that all genes known to be involved in unisexual flower development, such as *M* (*ACS2*), *A* (*ACS11*), *WIP1*, and *ACO2*, are expressed preferentially in the carpel primordia (Yamasaki et al., 2001; Boualem et al., 2008; Li et al., 2009; Martin et al., 2009; Boualem et al., 2015; Chen et al., 2016). Although there is no direct evidence for cucumber as to whether ethylene is required for carpel development, in tobacco (*Nicotiana tabacum*), it has been shown that ethylene is required for ovule development (De Martinis and Mariani, 1999).

Analysis of the pre-microRNA distribution in male, female, and hermaphrodite cucumber flowers suggested that ethylene is required for carpel development, by rescuing stress inhibition of carpel primordia (Sun et al., 2010). This ethylene-mediated inhibition of anther primordia development, in the female flower, might have been a side-effect of carpel rescue, and such an inhibition could well have been selected through advantages conferred by outcross pollination. In our previous study, we proposed that the *F* gene might have been co-opted, after the *M* and *A* genes, to a regulatory mechanism to enhance carpel development (Sun et al., 2010). From this perspective, clarification of the role played

by the *F* gene is central to deciphering the molecular mechanism of unisexual flower development, in cucumber; this would likely provide the last piece to complete the puzzle of the genetic FAM model.

In the present study, we sought to clarify the molecular basis of the *F* locus to provide a complete scenario for the FAM model of cucumber unisexual flower regulation, at a molecular level. To this end, we used a combination of CRISPR/Cas9 gene editing and ethyl methanesulfonate (EMS) mutagenesis to assess the functions of the genes within the *F* locus in determining female flower development. In addition, we transformed monoecious cucumber with the entire *ACS1G* genomic region and these lines became gynoecious. Our findings revealed that *ACS1G*, not *ACS1* or other genes in the *F* locus, is the gene responsible for development of female flowers. We further demonstrate that *ACS1G* is strongly expressed in every floral bud, at early stage 2, bypassing the need for *ACS11*, thereby establishing a dominant pathway for female floral development. This *ACS1G* expression pattern is conferred by the promoter of *ACS1G*. Based on these findings, we propose a model to explain how the various ethylene biosynthesis genes function to ensure successful carpel development in cucumber.

Results

F locus genomic structure

The *F* locus contains two annotated genes, *CsaV3_6G044400* (*ACS1*) and *CsaV3_6G044410*, and a part of *CsaV3_6G044420* (*Branched Chain Amino Acid Transaminase*, *BCAT*). *CsaV3_6G044410* encodes a cucumber MYB family transcription factor, hereafter identified as *MYB1*. In gynoecious

plants carrying the *F* locus, the entire *MYB1* region is duplicated. In addition, within this region, *ACS1G* gained a part of the *BCAT* gene, likely functioning as a distal promoter, but it retained the same proximal promoter, untranslated, and coding regions as *ACS1*. We also ascertained that the gynoecious lines (*FF* genotype) retained a complete copy of the *ACS1* and *BCAT* genes, as in the monoecious lines (Figure 1A).

Considering the complicated structure of the *F* locus, for clarity, we developed nomenclature to distinguish the genes in this region. *ACS1G* stands for the gynoecious-specific *ACS1* copy with a novel promoter; the *ACS1* copies on the *F* and *f* haplotypes are designated as *ACS1F* and *ACS1f*, respectively, and have identical genic and flanking sequences. However, *ACS1F* is always genetically linked to *ACS1G*. The *MYB1* copy in the *f* haplotype was named *MYB1f* and the two *MYB1* copies in the *F* haplotype were termed *MYB1a* (5' to *ACS1G*) and *MYB1b* (3' to *ACS1G*); these three *MYB1* copies have identical genic and flanking sequences (Figure 1A).

To explore the *F* gene identity, we first assessed the expression level, within floral buds, of the three candidate genes from near isogenic gynoecious and monoecious lines. *ACS1G* has a different promoter as both *ACS1F* and *ACS1G* share identical untranslated and coding sequences; therefore, we were unable to distinguish between their expression levels. Through RT-qPCR (Real-time Polymerase Chain Reaction) assays, we determined that *ACS1F/ACS1G* and *MYB1* had elevated expression levels in floral buds (pre-stage 4) from gynoecious compared to near-isogenic monoecious lines (Figure 1, B–D). Based on these expression profiles, we concluded that *BCAT* is unlikely to be the *F* gene (since its expression was unchanged between lines), but we could not discount the possibility that *MYB1* functions as the *F* gene.

Gynoecy requires a functional *ACS1G*

To assess the impact of *ACS1F*, *ACS1G*, *MYB1a*, and *MYB1b* on the gynoecious phenotype, we sought to generate loss-of-function mutations in each of these genes. The *FF* genotypes are recalcitrant to current transformation protocols (Hu et al., 2017); therefore, we employed a CRISPR/Cas9 gene-editing (CR) approach, using the transformable cucumber *ff* genotype, to generate loss-of-function *MYB1^{CR}* mutants. These transformed *T₀* seedlings were then used as the male parent and crossed with *FF* near-isogenic lines (Supplemental Figure 1, A and B). Pollen containing the *Cas9* transgenic fragment was next employed to generate *F₁* plants in which the target genes, located on the *F* haplotype, were further edited (Figure 2A). It is important to stress that, in the *F₁* plants, generated from pollen obtained from the transformed *T₀* seedlings but not containing *Cas9*, only the target gene located on the *f* haplotype was modified, as gene-editing occurred in the *T₀* generation of the *ff* genotype plants (Figure 2A; Supplemental Figure 1B).

In the 31 tested *F₁* plants not carrying *Cas9*, only *MYB1f* was mutated (*MYB1f^{CR}*, Figure 2A; Supplemental Figures 1, A and 2); in the 32 tested *F₁* plants carrying *Cas9*, each of

the three *MYB1* copies was mutated (*MYB1^{CR}*, Figure 2A; Supplemental Figures 1B and 3). Sequencing and sex phenotyping derived from 15 randomly selected seedlings are shown here (Figure 2C; Supplemental Figures 2 and 3). Given that both mutant types were gynoecious (Figure 2C), we could exclude *MYB1* as the *F* gene.

Similarly, we generated *Ff* plants with only mutated *ACS1f* (*ACS1f^{CR}*, Figure 2B; Supplemental Figures 1B and 4) or all copies of *ACS1* mutated (*ACS1^{CR}*, Figure 2B; Supplemental Figures 1B and 5). Here, *ACS1f^{CR}* remained gynoecious, whereas the *ACS1^{CR}* plants were identified as monoecious (Figure 2C). These findings indicated that either *ACS1F* or *ACS1G*, or both *ACS1F* and *ACS1G* together, in the *F* locus, conferred the gynoecey phenotype.

Since *ACS1F* and *ACS1G* have identical untranslated and coding sequences, and the distance on chromosome 6 between *ACS1F* and *ACS1G* is only 30.2 kb, it is hard to distinguish their function simply by using CRISPR/Cas9 (Clustered Regularly Interspersed Short Palindromic Repeats/Crispr associated protein 9) or RNAi methods. However, whether gynoecey is conferred by a simple dosage effect, caused by two copies of *ACS1*, or by a novel *ACS1G* promoter conferring a special expression pattern, is an important question.

To further distinguish the functions of *ACS1F* and *ACS1G*, we constructed an EMS mutation library based on the *Ff* genotype sub-gynoecious line. It is extremely difficult to acquire seeds of EMS-treated gynoecious or sub-gynoecious lines containing the *F* locus because they are much more sensitive to the effects of EMS than the monoecious lines. These lines rarely bear male flowers, and it is not possible to use the *Ag⁺* treatment to induce male flowers because this typically exacerbates the toxicity of the EMS and hinders seedling growth and flowering. In any event, we performed EMS mutagenesis on three different *Ff*-background cucumbers several times, screened 1,500 *M₁* plants, and obtained two nonsynonymous mutations, *ACS1f^{E353K}* and *ACS1G^{H164Y}*, from the *YB-Ff* and *09-Ff* backgrounds, respectively (Figure 3, A and B; Supplemental Figure 6, A and B).

These two mutations, located in nonconserved domains (Figure 3C), did not compromise either the sub-gynoecious phenotype (Figure 3D; Supplemental Figure 6C), or the *ACS1* enzyme activity of these mutant proteins in terms of ethylene production (Figure 3E; Supplemental Figure 6D). However, these two single-nucleotide polymorphisms (SNPs) provided us with an opportunity to distinguish transcripts from *ACS1f*, *ACS1F*, or *ACS1G*, at the key developmental stages when the majority of transcripts from the *F* gene would be expected, since it causes gynoecey.

To use these SNPs to look at transcript levels of these *ACS1* genes, RNA was extracted from early-stage female-destined floral buds (pre-stage 4) located at nodes 10 and above on *ACS1f^{E353K}*(*Ff*) and *ACS1G^{H164Y}*(*Ff*) mutant plants (Figure 3D). The mixed transcripts from *ACS1F*, *ACS1f*, and *ACS1G* were amplified, using primers common to their coding regions, and the PCR products were then cloned into a T-vector. At least 8 randomly selected positive clones were

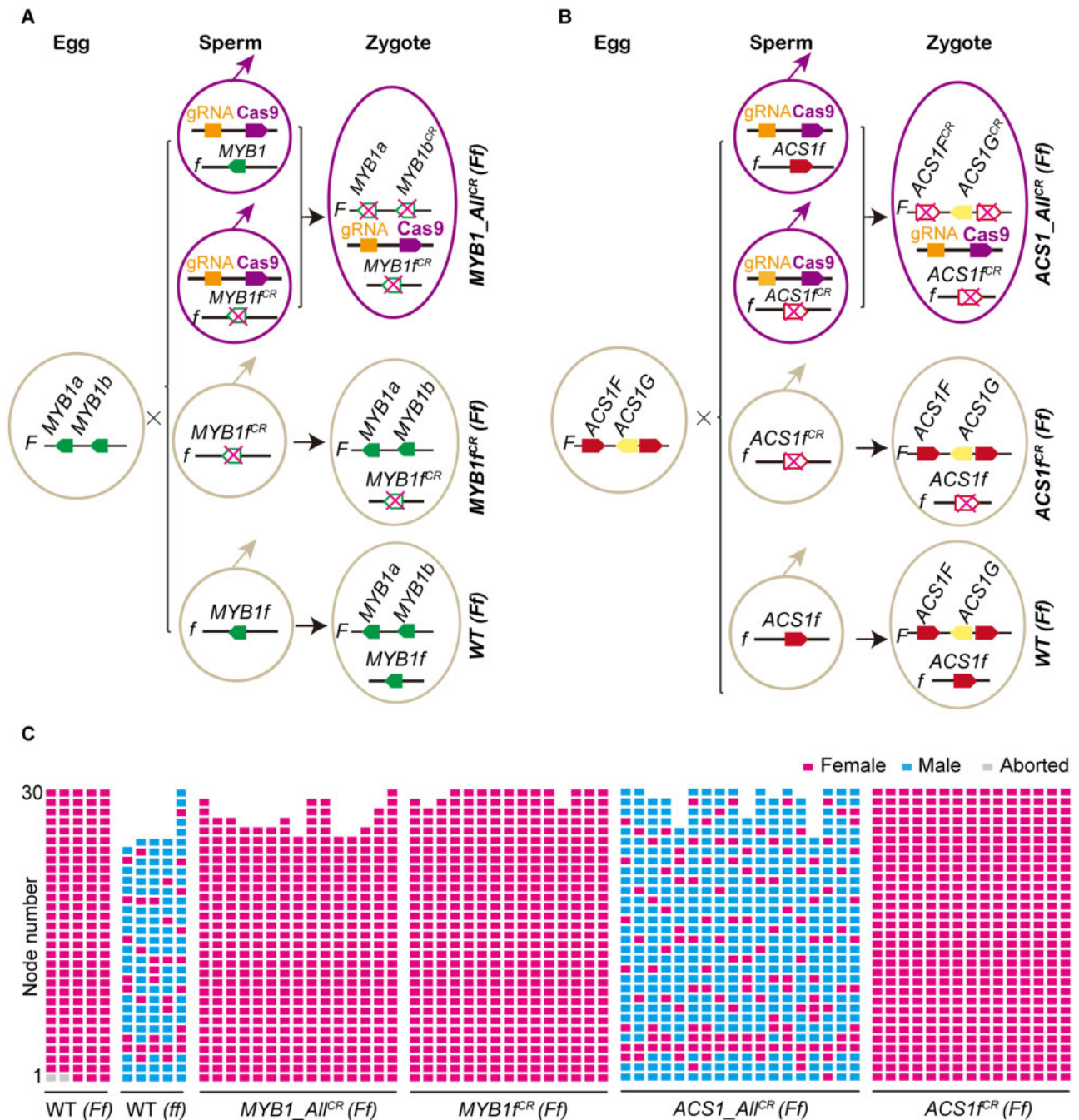


Figure 2 Genotypes and phenotypes of cucumber plants with CRISPR/Cas9-edited *MYB1* or *ACS1/1G*. (A and B) Schematic representation of the genotype of *MYB1_AII^{CR}*, *MYB1f^{CR}*, *ACS1_AII^{CR}* and *ACS1f^{CR}* with the *Ff* background. The sperm or zygote containing the *Cas9* transgenic fragments are marked in purple. Magenta crosses indicate the edited dysfunctional genes. In all plants containing the *Cas9* insertion, all copies of the target genes were mutated. (C) Graphic presentation of flower sex types in WT (*Ff*), WT (*ff*), *ACS1_AII^{CR}* (*Ff*), *ACS1f^{CR}* (*Ff*), *MYB1_AII^{CR}* (*Ff*), and *MYB1f^{CR}* (*Ff*). Each column represents an individual and each rectangle represents a node. Flower sex types are shown for at least 25 nodes. WT, wild-type.

sequenced for each plant, and at least 20 independent plants were analyzed for each mutant type. We next used the number of clones corresponding to the different SNPs to infer a ratio for the *ACS1F*, *ACS1f*, and *ACS1G* transcripts.

In the *ACS1f^{E353K}* (*Ff*) line, only wild-type transcripts were detected (Figure 3F), indicating that *ACS1f* was not expressed at the key floral developmental stage in the *Ff*

background. This finding indicated that *ACS1f* is not involved in promoting female floral development, consistent with the observation that *ACS1f^{CR}* (*Ff*) plants are gynoecious (Figure 2C).

As *ACS1f* was not expressed at the key developmental stage, in the *Ff* background, the *ACS1G^{HT64Y}* (*Ff*) line was used to distinguish transcripts from *ACS1F* (wild-type) and

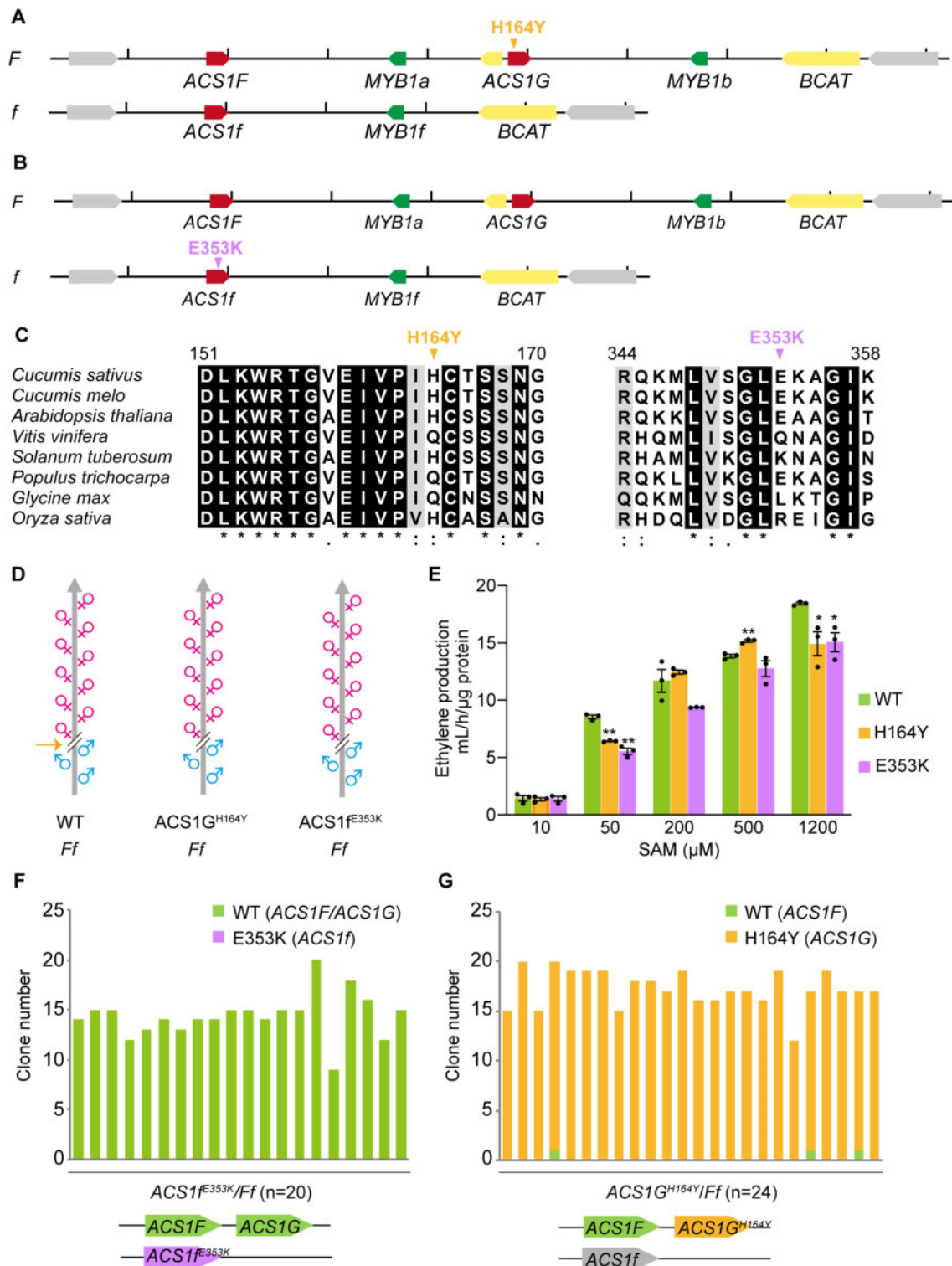


Figure 3 ACS1G transcripts are dominant in flowers at the key stage of female flower determination in gynocercous cucumber lines. (A and B) Schematic representation of the ACS1G^{H164Y} (A) and ACS1f^{E353K} (B) mutant genotypes with the *Ff* background. (C) Alignment of ACS1 homologous proteins from representative species. (D) The ACS1G^{H164Y} and ACS1f^{E353K} mutations did not affect the gynocercous flower sex types in the *Ff* background. Orange arrow indicates the boundary node between lower male nodes and upper female nodes, usually located at about node 10. (E) Enzymatic activity indicated by the ethylene production of wild-type ACS1/1G (green bars; WT), ACS1G^{H164Y} (orange bars) and ACS1f^{E353K} (purple bars) protein isoforms at various concentrations of SAM. Data are presented as mean \pm SE, $n = 3$. * $p < 0.05$ and ** $p < 0.01$ in Student's *t*-test compared to the wild-type ACS1/1G protein isoform (Statistical data are provided in Supplemental Data Set 1). (F) Number of T-clones containing WT and ACS1f^{E353K}-type transcripts in the ACS1f^{E353K} mutant line with the *Ff* background. A total of 20 individuals was analyzed, and for every individual at least 8 independent T-clones were sequenced to identify the SNP. (G) Number of T-clones containing WT ACS1F and ACS1G^{H164Y} in the ACS1G^{H164Y} mutant line with the *Ff* background. A total of 24 individuals was analyzed, and for every individual at least 12 independent T-clones were sequenced to identify the SNP.

ACS1G (H164Y SNP) plants. Our sequencing results revealed that during key stages determining the female flower, the major transcripts were derived from the ACS1G allele (Figure 3G); ACS1F transcripts were detected in only 3 of 24 plants, equating to 3 of 411 clones. In the independent 6 ACS1F^{WT}ACS1G^{H164Y}ACS1f^{E353K}(*Ff*) plants acquired from the cross between ACS1f^{E353K}(*Ff*) and ACS1G^{H164Y}(*Ff*) mutant plants (Supplemental Figure 7, A and B), the ACS1F clone was detected only once in a total of 65 clones (Supplemental Figure 7C), whereas all the other clones were ACS1G^{H164Y}. These findings provided strong support for the hypothesis that ACS1G is the *F* gene.

To further test our hypothesis that ACS1G is the *F* gene, we generated transgenic monoecious cucumber expressing the entire ACS1G genomic region, including a 4.5-kb region upstream from the start codon. Compared to the untransformed cucumber *ff* genotype (Figure 4B), expression of this ACS1G genomic region resulted in a gynoecious phenotype (Figure 4, A, C, and D). These findings established that ACS1G alone is necessary and sufficient to confer gynoecey in cucumber.

The novel ACS1G promoter confers a new expression pattern and female-promoting function

Next, we asked whether the female promotion function of ACS1G is conferred by a simple dosage effect of multiple copies of ACS1, or alternatively, by a new expression pattern due to its promoter. To explore these possibilities, we first performed in situ hybridization assays to monitor the expression pattern of ACS1G (Figure 5, A–C; Supplemental Figure 8, A–E). Given that, transcripts in the developing *Ff* floral buds, at pre-stage 4, were derived predominantly from ACS1G (Figure 3G), we reasoned that in situ hybridization, based on *FF* genotype plants, would reflect the expression

pattern of ACS1G, rather than that of ACS1F. Here, our assays revealed that ACS1G was expressed mainly during the early stages 1 and 2 of floral development (Figure 5, A and B; Supplemental Figure 8, A and B). At stage 2, ACS1G was expressed just beneath the central zone of the floral meristem, the region that can later develop into the carpels (Figure 5B). At stage 4, weak ACS1G signals were detected in the developing petal, stamen, and carpel primordia (Figure 5C; Supplemental Figure 8C). In monoecious cucumber (*ff* genotype), we detected no specific ACS1f expression pattern in floral bud stage 1 or 2 (Figure 5, D and E; Supplemental Figure 8, K and L). However, ACS1f was weakly expressed later, at stage 4 (Figure 5F; Supplemental Figure 8M).

To address whether these two expression profiles were conferred by the different promoters of ACS1G and ACS1f, we next generated *ProACS1G:GUS* and *ProACS1f:GUS* transgenic plants. GUS (β -glucuronidase) staining assays established that, from stages 1 to 3, the ACS1G promoter was expressed strongly (Figure 6, A–D); however, in the *ProACS1f:GUS* transgenic floral buds, at stages 1–3, no GUS signal was detected (Figure 6, E–H). These patterns are similar to those obtained by in situ hybridization.

In later floral development, at stages 4–8, the *ProACS1G:GUS* remained active within the lower region of the floral bud (Supplemental Figure 9, A–D), whereas *ProACS1f:GUS* generated only a weak GUS signal (Supplemental Figure 9, E–H). This *ProACS1G:GUS* pattern differed somewhat from that observed by in situ hybridization. This might reflect more distant *cis*-elements regulating the ACS1G expression, at these later developmental stages, which may be absent from our *ProACS1G:GUS* construct. In any event, collectively, these findings support the conclusion



Figure 4 Cucumber transgenic lines expressing the ACS1G genomic region exhibit the transition from monoecy to gynoecey. (A) Flower sex type of transgenic CU2 (*ff*) carrying the ACS1G genomic region. Scale bar = 10 cm. (B) Flower sex type of CU2 (*ff*). Scale bar = 10 cm. (C) Genomic verification of the transgenic fragments using primers for the right border. (1) transgenic CU2 plant expressing the ACS1G genomic region; (2) CU2; (3) plasmid as the positive control. (D) Genomic verification of the transgenic fragments using primers for *bar*, an antibiotic selection gene. (1) transgenic CU2 plant expressing the ACS1G genomic region; (2) CU2; (3) plasmid as the positive control.

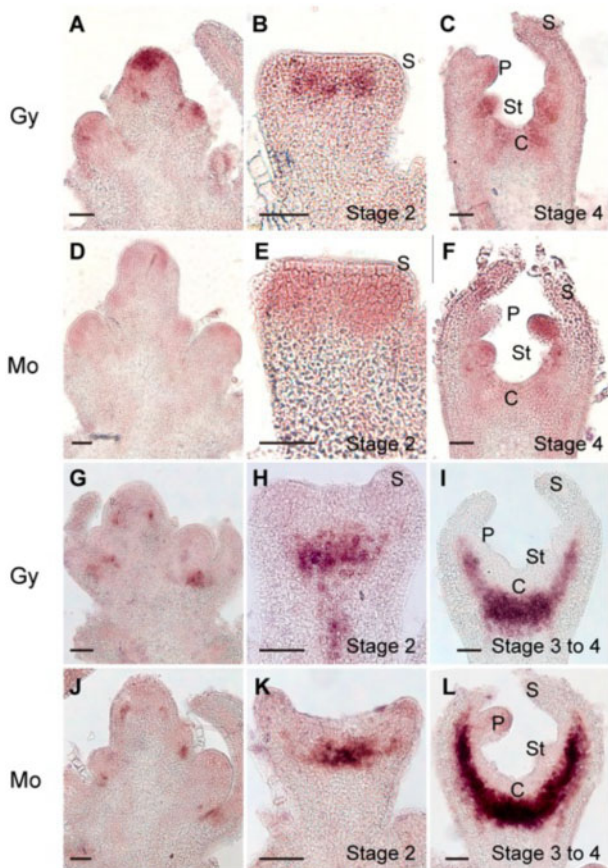


Figure 5 Expression patterns of *ACS1G*, *ACS1f* and *ACO2* in early-stage floral buds in the indicated cucumber lines. (A–F) In situ hybridization of *ACS1G* in gynoecious (Gy) (A–C) and *ACS1f* in monoecious (Mo) (D–F) floral buds. (G–L) In situ hybridization of *ACO2* in floral buds of gynoecious (G–I) and monoecious (Mo) (J–L) lines. (A, D, G, and J) A shoot apex containing floral buds in early development. (B, E, H, and K) Floral buds in early stage 2 of development. (C and F) Floral buds at developmental stage 4. (I and L) Floral buds at developmental stages 3–4. S, sepal; P, petal; St, stamen; C, carpel. Scale bars = 50 μ m.

that a recombination in the cucumber genome gave *ACS1G* a new promoter and function.

Genetic relationship among the genes involved in determining the ratio of unisexual flowers

In monoecious cucumber, *Androecious* (A) is encoded by *ACS11*, which is expressed specifically in the carpel regions of floral buds destined to be female, where it cooperates with *ACO2* to release the ethylene essential for initiating the female developmental pathway (Boualem et al., 2015; Chen et al., 2016). In contrast, in the presence of the *F* locus, *ACS1G* predominates during female flower development and confers gynoecy whether *ACS11* is functional or not; this condition has been described as epistasis of the *F* gene over the *a* allele (Kubicki, 1969a, 1969c). Considering that both *ACS1G* and *ACS11* encode ACS, if *ACS1G* has the potential

to release ethylene, at the right time and within the right position, then this epistasis can be explained.

The patterns of *ACS11* and *ACO2* expression overlapped at stage 4 in the flower buds determined to be female (Boualem et al., 2015; Chen et al., 2016). To determine whether *ACS1G* could cooperate with *ACO2* to release the ethylene essential for female flower promotion, thus taking the place of *ACS11*, we next analyzed the *ACO2* expression pattern. In the *FF* gynoecious line, *ACO2* was strongly expressed in the central region of the stage-2 floral bud (Figure 5H; Supplemental Figure 8, F–H) and overlapped with the *ACS1G* expression domain (Figure 5B). However, in the monoecious cucumber (*ff* genotype), overlapping expression of *ACS1f* and *ACO2* was not observed at these key stages when the flower sex type is determined (Figure 5, D–F, J–L; Supplemental Figure 8, K–P). These findings provided support for the hypothesis that the female-promoting function of *ACS1G* arises from its overlapping expression domain with *ACO2*, and their cooperation to generate the prerequisite ethylene burst.

We next investigated whether the *ACS1G/aco2/aco2* genotype plants (where *ACS1G/* includes *ACS1G/ACS1G* and *ACS1G/acs1g*) could produce female flowers. *ACS1G* is linked to *ACO2* on chromosome 6, with a physical distance of 2 Mb. Of 187 F_2 plants obtained from a cross between YB-Gy (*ACS1G/ACS1G ACO2/ACO2*) and 406a (*acs1g/acs1g aco2/aco2*), all nine *ACS1G aco2/aco2* genotype plants were androecious (Table 1). This result is consistent with our earlier findings that the application of ACC does not rescue the androecious phenotype of the *aco2* homozygous mutants (Chen et al., 2016) and demonstrated that *F* gene function is dependent on *ACO2* and, further, that *ACS1G* must cooperate with *ACO2* to produce the required ethylene dosage. Based on these findings, we concluded that the spatial and temporal expression pattern of *ACS1G*, rather than a simple dosage effect of *ACS1* due to copy number variation, confers the female promoting function of *ACS1G*.

Loss-of-function mutations in *WIP1* also promote female flowers in cucurbits (Martin et al., 2009; Hu et al., 2017; Zhang et al., 2020). Furthermore, *WIP1* expression is repressed by *ACS11* expression in cucumber and melon (Boualem et al., 2015). Therefore, we next investigated whether *ACS1G* expression and ethylene production repress *WIP1* expression. Compared with the isogenic monoecious lines, *WIP1* expression was reduced significantly in the gynoecious lines (Figure 7A). In addition, treatment with ethephon, which is converted into ethylene, also significantly downregulated *WIP1* expression (Figure 7B). Furthermore, *ACS2* expression was up-regulated dramatically in the gynoecious plants that lack a functional *WIP1* (Figure 7C). Based on these findings, the epistasis of *F* (*ACS1G*) over *a* (loss-of-function of *ACS11*) can be explained as follows: *ACS1G* is expressed in every floral bud and cooperates with *ACO2*, bypassing the need for *ACS11*, to release ethylene, which represses *WIP1* expression and upregulates *ACS2*, leading to all floral buds being programmed to be female (Figure 7D).

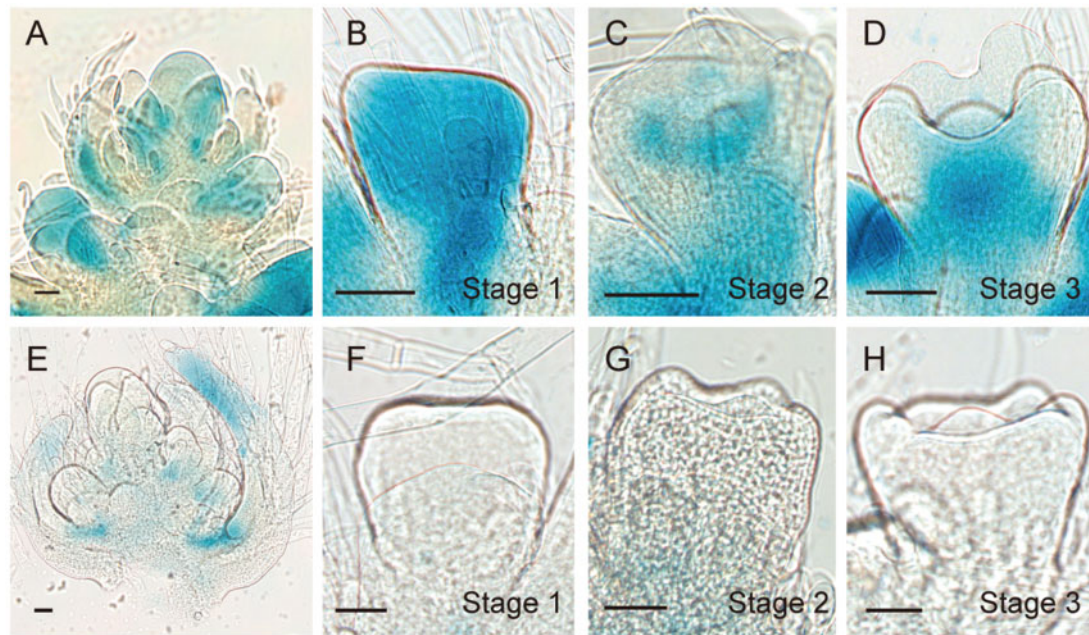


Figure 6 GUS staining pattern in stages 1–3 floral buds of *proACS1G:GUS* and *proACS1f:GUS* transgenic cucumber lines. (A–D) GUS detection in floral buds of *proACS1G:GUS* transgenic plants. (E–H) GUS detection in floral buds of *proACS1f:GUS* transgenic plants. (A and E) A shoot apex containing floral buds in early development. (B and F) Floral buds in stage 1 development. (C and G) Floral buds in stage 2 development. (D and H) Floral buds in stage 3 development. Scale bars = 50 μm .

Table 1 Genotypes and phenotypes of the plants of F_2 populations derived from crosses between *ACS1G ACS1G ACO2ACO2* and *acs1-gacs1g aco2aco2*. **Bold values are the number of the *ACS1G_aco2/aco2* seedlings, which could show the genetic relationship between *ACS1G* and *ACO2*.**

Genotype	Phenotype	No. of plants
<i>ACS1G_ ACO2/ACO2</i>	Sub-gynoecious	38
<i>ACS1G_ ACO2/aco2</i>	Sub-gynoecious	87
<i>acs1g/acs1g aco2/aco2</i>	Androecious	32
<i>ACS1G_ aco2/aco2</i>	Androecious	9
<i>acs1g/acs1g ACO2/aco2</i>	Monoecious	10

Discussion

New technology provided the opportunity to complete the puzzle of the FAM model

The *ACS1G* gene was the first ethylene biosynthesis gene reported to be linked with the gynoecy phenotype in the FAM model (Trebitsh et al., 1997). However, due to the complexity of the *F* locus genome structure (Zhang et al., 2015), definitive evidence demonstrating that *ACS1G* is responsible for female flower determination, as opposed to other genes within the *F* locus, was lacking. Furthermore, a full molecular dissection of the *F* locus is essential for understanding unisexual flower development in cucumber.

In this study, we demonstrate that only *ACS1G*, not *BCAT*, *MYB1a/b* or *ACS1*, functions as the *F* gene (Figures 1–4). In addition, we discovered that the *ACS1G* expression pattern was created by a combination of the *BCAT* intron and the *ACS1*-coding sequence. Expression driven by this promoter resulted in *ACS1G* acquiring dominance over other ethylene

synthesis genes, in regulating female flower development. Thus, we have now obtained the final molecular information to complete the puzzle of the FAM model.

It is intriguing that it took two decades to establish that *ACS1G* is the functional gene of the *F* locus. Naturally, in the absence of an annotated cucumber genome, the complex structure of the *F* locus represented a significant challenge. As an example, the presence of *MYB1*, in the *F* locus, was not revealed until 2015 (Zhang et al., 2015). Next, downregulation of *ACS1/ACS1G*, based on RNAi, could transform gynoecious into monoecious lines (Shiber et al., 2008). However, as these two genes share identical untranslated and coding regions, a functional analysis of each gene was impossible to achieve through RNAi. Finally, the other genes in the *F* locus, such as *ACS1*, *MYB1a*, and *MYB1b*, as well as *BCAT*, are tightly linked with *ACS1G*, and hence, their segregation from *ACS1G* was not possible. With the advent of CRISPR/Cas9 gene editing technology, we were able to use this method, in combination with an EMS mutant library, to identify mutations that allowed us to test, directly, whether *ACS1* or *ACS1G* functions as the *F* gene.

Identification of *ACS1G* as the *F* gene revealed an interesting situation in that all players in the FAM model are different members of the ACS gene family. Interestingly, previous efforts to discover the identity of the FAM genes uncovered two players in the regulation of female flowers, namely *ACO2* and *WIP1* (Martin et al., 2009; Chen et al., 2016; Hu et al., 2017). Here, *ACO2* is a key enzyme in the ethylene biosynthesis pathway, while *WIP1* is repressed by *ACS11* (A gene), which relieves its repression of *ACS2* (M gene; Boualem et al., 2008, 2015). This raises the

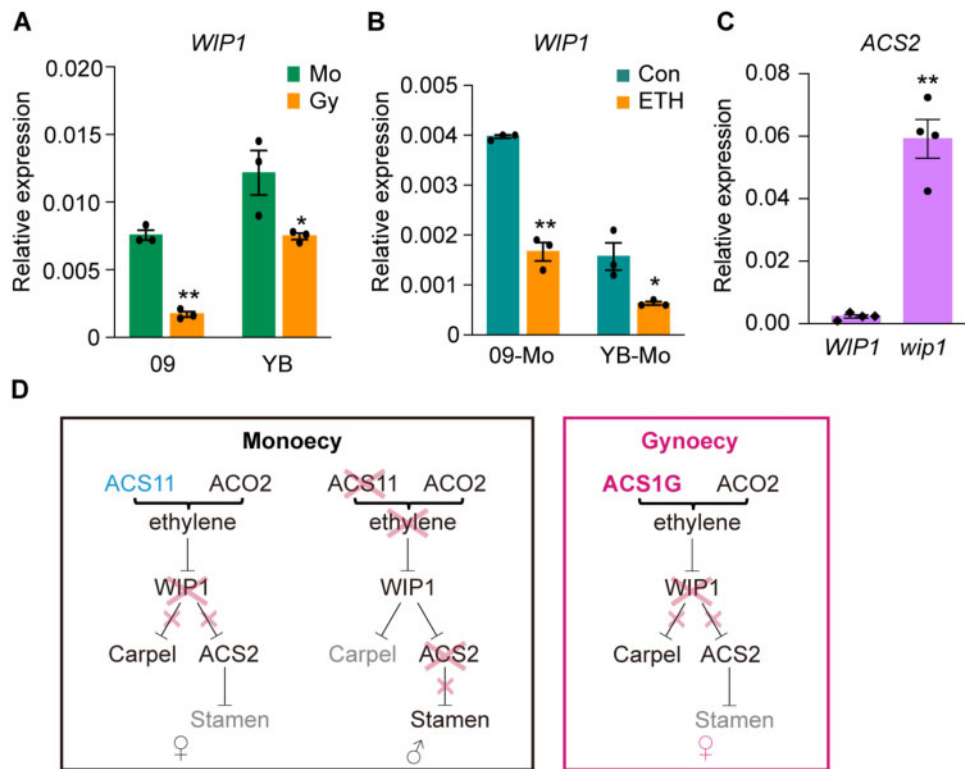


Figure 7 Expression levels of *WIP1* and *ACS2* in the apices of cucumber isogenic lines. (A) *WIP1* expression in gynoecious (Gy) and monoecious (Mo) isogenic lines. Mo, monoecious; Gy, gynoecious. “YB” and “09” are two different genetic backgrounds. Data are presented as mean \pm SE, $n = 3$. * $p < 0.05$ and ** $p < 0.01$ in Student’s t -test compared to the isogenic monoecious lines (Supplemental Data Set 1). (B) *WIP1* expression in shoot apices of monoecious lines. Con, control, treated with water; ETH, treated with ethephon. Data are presented as mean \pm SE, $n = 3$. * $p < 0.05$ and ** $p < 0.01$ in Student’s t -test compared to the control (Supplemental Data Set 1). (C) *ACS2* expression in shoot apices of monoecious CU2 (*WIP1WIP1* genotype) and gynoecious CU2 (*wip1wip1* genotype) lines. Data are presented as mean \pm SE, $n = 4$. * $p < 0.05$ and ** $p < 0.01$ in Student’s t -test compared to CU2 (*WIP1WIP1*) genotype (Supplemental Data Set 1). (D) Model for regulating gynoecy and monoecy in cucumber.

rhetorical question of why might the ethylene synthesis genes have been selected to play a pivotal role in female flower development? Furthermore, it is intriguing to ponder what series of events led to the involvement of multiple ACS genes, and what might control the interaction between these genes? Answers to these questions can be sought through interrogation of the extensive cucurbit genomics databases, which includes genetic diversity from undomesticated and landrace accessions to commercial cultivars.

Differences between the Female (*F*) and gynoecy (*g*) genes

Although both the *F* and *g* genes promote female flower formation, there are important differences. The *F* gene (*ACS1G*) is dominant, and it has been discovered only in cucumber, but not in other cucurbit species. However, the *g* gene (dysfunctional *WIP1*) is recessive, and its function is conserved in melon, cucumber, and watermelon (Martin et al., 2009; Hu et al., 2017; Zhang et al., 2020). In addition, the *wip1* mutants bear some bisexual flowers, at the lower nodes, but cucumbers carrying the *F* locus produce no bisexual flowers.

To further an understanding the genetic relationship between *F* and *WIP1*, we obtained $F_- wip1$ seeds (where F_-

can be FF or Ff) from an F_2 population derived from a cross between $CU2-FF$ and our *wip1* mutants (CRISPR/Cas9 edited). As with cucumbers containing the *F* locus, these $F_- wip1$ plants produced female, but no bisexual flowers (Supplemental Figure 10). This established that the ethylene, produced by *ACS1G* and *ACO2*, could activate *ACS2* expression, not only by repressing *WIP1* expression, but also through another *WIP1*-independent pathway (Supplemental Figure 13D). Of note here, in *Cucurbita pepo*, female flowers can be produced when *WIP1* expression is not downregulated (Garcia et al., 2020), which is consistent with the notion that other pathways must exist to overcome the repression of *CpACS27* (ortholog of *ACS2* and *ACS7*) by *WIP1*. Identification of the factors that participate in such pathway(s) will be the focus of future studies.

As we mentioned above, the *F* gene is epistatic to the *a* gene, which means that $F acs11$ plants are gynoecious (Kubicki, 1969a, 1969c). In the present study, we demonstrated that $F aco2/ac02$ is androecious. To further our understanding of the differences between the two female promoting genes, *ACS1G* and *wip1*, we obtained the *wip1 acs11* (from an F_2 population between *wip1* and Erez) and *wip1 aco2* (from an F_2 population between *wip1* and 406a) double mutants. Similar to the findings in melon, these *wip1*

acs11 double mutants produced both bisexual and female flowers, like the *wip1* single mutant (Supplemental Figure 11). These findings indicate that, in cucumber, *WIP1* also functions downstream of *ACS11*. However, the *wip1 aco2* double mutants produced bisexual, but not female, flowers (Supplemental Figure 12, A–D). Furthermore, RT-qPCR assays showed that *ACS2* was not upregulated significantly in these *wip1 aco2* double mutant plants (Supplemental Figure 12E). Hence, the downregulation of *WIP1*, or dysfunctional *WIP1*, is not sufficient to activate *ACS2* expression, and functional *ACO2* is necessary for activating *ACS2* expression.

The need for *ACO2* to activate *ACS2* expression and ensure female flower formation in the *wip1 aco2* double mutant is difficult to reconcile with the current model. If *ACO2* cooperates with *ACS11* in repressing *WIP1* and upregulating *ACS2*, then the *wip1 aco2* and *wip1 acs11* plants should have similar phenotypes. Thus, another ACS could cooperate with *ACO2* to release the ethylene in these *wip1 acs11* double mutants, but this ACS gene would be repressed by *WIP1* in monoecious cucumber. Whether *ACS2* is a candidate, or if another ACS could perform this function remains to be determined.

New model of unisexual flower development in cucumber

The question as to which specific ethylene synthesis genes interact in flower development is addressed by our current spatiotemporal examination of the expression patterns of *ACS1G*, *ACS1*, and *ACO2* (Figure 5), when assessed together with known *ACS2*, *ACS11*, as well as *WIP1*, expression patterns (Saito et al., 2007; Boualem et al., 2008, 2015; Li et al., 2009; Martin et al., 2009). Previous evidence indicated that, during carpel development, *ACO2* functions as a basal player, regardless of whether a floral bud is male or female (Chen et al., 2016). In addition, for lines lacking the *F* locus, after floral buds have developed to stage 4, when *ACO2* is expressed along the receptacle (Supplemental Figure 13A), the *ACS11* (*A* gene) is expressed in some floral buds, which then represses *WIP1* expression, thereby activating *ACS2* (*M* gene) expression (Martin et al., 2009; Boualem et al., 2015). In this situation, these floral buds are developmentally programmed to become female. However, in those floral buds in which *ACS11* is not being expressed, the male developmental program is active. In this way, the presence or absence of *ACS11* activity leads to the monoecious phenotype, in that both female and male flowers are produced on the same plant (Figure 7D).

An elimination of *ACS11* function, as in the *aa* genotype (Boualem et al., 2015), or of *ACO2* function (Chen et al., 2016), will cause *WIP1* repression to be released, and as a consequence, *ACS2* (*M* gene) expression is repressed, thereby giving an insufficient ethylene level to activate carpel development; the result is male floral bud development (Supplemental Figure 13B). In contrast to the regulatory roles of *ACS11* (*A* gene) and *WIP1*, the *ACS2* (*M* gene)

appears to be the last player in the *FAM* regulatory system. In any event, with functional *ACS2* expression, regardless of the reason, there will be sufficient ethylene for carpel development, and so the floral bud will develop as female. In the situation in which *ACS2* is lacking, carpel development occurs only when both *ACO2* and *ACS11* provide marginal, but sufficient ethylene, to meet the requirement for carpel development: this level of ethylene does not arrest stamen development, and thus, the flowers are bisexual (Supplemental Figure 13C). In this regard, *WIP1* and *ACS11* may be coopted, through a regulatory complex, to regulate or stabilize *ACS2* expression, a basic requirement for carpel development.

The *F* gene (*ACS1G*) functions uniquely in that it is expressed only in lines carrying the *F* locus, and it is expressed as early as *ACO2*, at bud stage 2 (Figures 5 and 7, D; Supplemental Figure 13D). In the homozygous background, *ACS1G* expression in the floral buds gives rise to female flowers, regardless of the existence of *ACS11* (*A* gene). These findings indicate that *ACS1G* can bypass the need for *ACS11* and work directly with *ACO2* to upregulate *ACS2* and thereby ensure carpel development (Figure 7D); in this way, *ACS1G* exhibits dominance over *ACS11*. Here it should be mentioned that, at times, the genetic data offer only a potential regulatory framework, and thus, biochemical experiments may be needed to provide the detailed relations between the involved components, or elucidate other possibilities for the underlying gene interactions.

Identification of additional factors controlling expression patterns of ACS genes is needed for an understanding of unisexual flower development

The dominance of *ACS1G* over other ACS genes implies that these different members might be co-opted, in a stepwise manner, dependent upon the requirement for carpel development; here, the robustness of the rescuing mechanism might well contribute to its selection. This observed *ACS1G* dominance may reflect its duplication origin, and is consistent with the hypothesis that it is the newest integration of an ACS gene family member into the regulatory complex for cucumber carpel development (Sun et al., 2010).

Currently, we know that, in monoecious cucumber, selective expression of *ACS11* triggers female flower development, whereas in gynoeious cucumber, *ACS1G* dominates in female flower development. Irrespective of whether the cucumber line is monoecious or gynoeious, upregulation of *ACS2* is essential for female flower development. Clearly, gaining an understanding of the regulatory system that controls *ACS11*, *ACS1G*, and *ACS2* expression would advance our understanding of unisexual flower development. Except for expression in the carpel region, *ACS11* is also expressed in the underlying phloem of the female floral bud. This raises the question as to whether there might be factors, delivered via the phloem, which could serve to integrate both physiological and environmental inputs to impact the local

decision on floral bud development, as to whether to produce male or female flowers.

ACS1G is expressed at a very early stage in the carpel of every floral bud. The mechanism by which this new gene, ACS1G, acquired this novel function, within an already existing transcriptional regulatory network, needs to be elucidated in future studies. Finally, although WIP1 is a repressor of ACS2, it seems there are still other pathways and factors that can regulate ACS2 expression. Identification of such additional factors that can regulate ACS expression patterns, thereby leading to unisexual flowers development, should advance our understanding of the mechanisms regulating unisexual flower development in the cucurbits.

Materials and methods

Plant materials and growth conditions

Seeds of the three pairs of isogenic cucumber (*Cucumis sativus* L.) inbred lines, CU2-Gy (Gynoecious, FFMM) and CU2-Mo (Monoecious, ffMM); YB-Gy (Gynoecious, FFMM) and YB-Mo (Monoecious, ffMM); 09-Gy (Gynoecious, FFMM) and 09-Mo (Monoecious, ffMM) were obtained from Hunan Xingshu Seed Industry Co., Ltd. (Chang Sha, Hunan, China). EMS-induced mutants were based on the YB and 09 backgrounds. Requests for these EMS-induced mutants require a material transfer agreement with Hunan Xingshu Seed Industry. If the proprietary inbred line is requested, then Hunan Xingshu Seed Industry will provide a hybrid, derived from the requested inbred, at its discretion. Seeds of the inbred line CU2-Mo were used for transformations. The CU2-Gy lines were crossed with the transgenic lines with a background of CU2-Mo. Floral buds from YB-Gy, YB-Mo, 09-Gy, and 09-Mo plants, at the six-leaf stage were used for gene expression analyses. All plants were grown in a greenhouse at the Institute of Vegetables and Flowers, Chinese Academy of Agricultural Sciences, Beijing, China.

Reverse transcription quantitative PCR analyses

Shoot tips were collected from seedlings, at the six-leaf stage, and floral buds before stage 4 were dissected under a microscope. For each RNA sample (biological replicate), floral buds from at least five seedlings were mixed and total RNA was isolated using Trizol reagent (Thermo Fisher Scientific, Waltham, MA, USA; #15596-026). Total RNA was further digested with DNaseI (Takara Bio, Kusatsu, Japan; #2270A) and reverse transcribed into cDNA using TransScript One-Step gDNA Removal and cDNA Synthesis SuperMix (Tiangen Biotech, Beijing, China; AT311), according to the user manual. Quantitative PCR analyses were performed using SYBR Premix ExTaq Mix (Takara Bio; #RR420A) and an ABI7500 PCR System (Thermo Fisher Scientific), according to the manufacturer's instructions. The relative expression of each target gene was calculated according to the comparative C_T method (Schmittgen and Livak, 2008), using *ACTIN2* (*CsaV3_6G041900*) as a reference. Three technical replicates were used to calculate the C_T value, and at least three biological replicates were analyzed.

For each biological replicate, four to five shoot tips, containing the flower buds before stage 7, were mixed. Primer design was performed using Primer Premier 5 software (Premier Biosoft, Palo Alto, CA, USA). Primer sequences are listed in Supplemental Table 1.

CRISPR/Cas9 vector construction

To ensure mutation of a target gene, two gRNAs were employed. The pCBC-DT1T2 vector (Xing et al., 2014) was used as the template; MYB-gRNA1-F and MYB-gRNA2-R primers were used to amplify the PCR fragment containing the two gRNAs for targeting *MYB1*; ACS1-gRNA1-F and ACS1-gRNA2-R primers were used to amplify the PCR fragment containing the two gRNAs for targeting *ACS1*. The resultant purified PCR fragments were inserted, separately, into the vector pKSE401, containing *Pro35S::GFP* (Hu et al., 2017), using In-Fusion HD Cloning Plus (Clontech, #638909) (reaction time of 30 min at 50°C). The clones pKSE401-2sgRNA-MYB1 and pKSE401-2sgRNA-ACS1 were confirmed by sequencing and then transformed into *Agrobacterium tumefaciens* strain EHA105 for cucumber transformation. PCR primer sequences are listed in Supplemental Table 2.

Cucumber transformation

Cucumber transformation was performed as previously described (Hu et al., 2017). Briefly, the seeds of the inbred line CU2 were peeled and sterilized, then germinated on Murashige and Skoog medium containing 2 mg/L 6-benzylaminopurine (BA) and 1 mg/L abscisic acid (ABA) for 2 days in the dark at 28°C. Explants were prepared by removing the germ and transverse cutting of the cotyledon. The verified vector was introduced into the *A. tumefaciens* strain EHA105, and transformed clones were incubated, overnight, in Luria-Bertani medium containing 50 mg/L kanamycin and 25 mg/L rifampicin, at 28°C, then incubated in 30 mL LB medium until the culture OD_{600} (the optical density of a sample measured at a wavelength of 600 nm) reached 0.4–0.8. The cell culture was then collected by centrifugation and diluted in inoculation medium (MS medium containing 2 mg/L BA, 1 mg/L ABA, 200 μ M acetosyringone, and 10 mM MES [pH 5.2]) to an OD_{600} of 0.2. The explants were then immersed in 10 mL inoculation medium, contained within a 20-mL syringe, and vacuum infiltration was performed by pulling up on the plunger. After the infection, explants were co-cultured with the *Agrobacterium* on three layers of damp filter papers for ~72 h, in the dark, then washed with sterilized water and transferred to the shoot regeneration medium (2 mg/L BA, 1 mg/L ABA, 100 mg/L kanamycin, and 200 mg/L timentin).

Shoots appeared in 3–4 weeks, and the transformed buds were selected by screening for GFP (Green Fluorescent Protein) fluorescence. These transgenic buds were excised from the explants and planted onto elongation MS medium (1.0 mg/L gibberellic acid, 0.1 mg/L BA, 0.01 mg/L 1-naphthaleneacetic acid, 2 mg/L AgNO₃, and 100 mg/L timentin), and cultured at 25°C until they reached ~4 cm, at which time shoots were transferred onto rooting medium (6.5 mg/

L hemin and 100 mg/L timentin). Successfully rooted seedlings were cultured for 5 days under low light and then transplanted to soil. Transgenic constructs were verified using PCR and by monitoring GFP fluorescence at later growth stages.

EMS mutagenesis and targeting induced local lesions in genomes (TILLING)

EMS mutagenesis and a targeting induced local lesions in genomes (TILLING) screen were performed, as previously described (Tadmor et al., 2007), with some modifications to meet the needs of isolating mutations in the region of the *F* locus. Since the gynoecious lines with the *FF* background rarely form male flowers, and were particularly susceptible to the effects of EMS, seeds with the 09-Ff and YB-Ff backgrounds, from the crosses between 09-Gy and 09-Mo, and YB-Gy and YB-Mo, were used for the EMS mutagenesis, thereby allowing the use for self-pollination of male flowers that developed at the lower nodes. This circumvented the need for the AgNO₃ treatment to induce male flowers, which is known to severely aggravate the growth and infertility issues in EMS-treated plants. Because the *F* locus is a genomic duplicated region, the ratio of point mutations was difficult to detect from a sampling pool of the M₂ population. Instead, a TILLING screen was applied to the fertile M₁ plants. For each M₁ plant containing a mutation in the screened region of interest, the PCR products were sequenced to verify the mutation type; each M₂ individual generated from the self-pollination of these M₁ plants was then analyzed to determine its homo- or heterozygosity for this mutation.

The leaf closest to the first fruit in each M₁ plant was collected and its genomic DNA was extracted. Primers covering the entire coding region of *ACS1/ACS1G* (Supplemental Table 2) were used for PCR amplification. After denaturation and annealing, the PCR products were digested with CEL I (Colbert et al., 2001) and analyzed using polyacrylamide gel electrophoresis. The M₂ population, generated from the M₁ plants containing mutations in *ACS1/ACS1G*, was used to assess whether the mutations were linked to the *F* locus. The specific primers used to identify the *F* locus are listed in Supplemental Table 2. Mutations not linked to the *F* locus were considered to be located in *ACS1f*. The possibility that the mutations in *ACS1F* or *ACS1G* were linked to the *F* locus was investigated by sequencing the amplification products with primers specific to the distal promoters of *ACS1F* and *ACS1G* (Supplemental Table 2). The homozygous and heterozygous alleles were estimated from the sequencing chromatograms, and then verified using the derived cleaved amplified polymorphic sequence (dCAPS) method (Neff et al., 1998). Primers for dCAPS are listed in Supplemental Table 2.

The M₂ plants containing *ACS1G*^{H164Y} and *ACS1f*^{E353K} mutations were backcrossed, individually, with 09-Mo (*ff*) and YB-Gy (*FF*). The offsprings (M₃ plants) were genotyped to select *ACS1G*^{H164Y} (*Ff*) and *ACS1f*^{E353K} (*Ff*) lines for

further analysis; the segregation ratio was determined using this generation.

Expression and purification of recombinant ACS1 isoforms

Coding sequences for the wild-type *ACS1*, *ACS1G*^{H164Y}, and *ACS1f*^{E353K} isoforms were introduced into the pET30a (Merck Millipore, Burlington, MA, USA) plasmid. The constructs were verified by sequencing and then individually transformed into the BL21 (DE3) *Escherichia coli* strain. Transformants were placed in LB medium supplemented with kanamycin (50 mg/L) and incubated overnight at 37°C, with shaking at 200 r.p.m. The pre-culture cells were incubated in 500 mL LB medium containing 50 mg/L kanamycin and were shaken at 37°C until the culture had an OD₆₀₀ of 0.6. Isopropyl β-D-1-thiogalactopyranoside was then added to a final concentration of 0.05 mM. After shaking the culture at 180 r.p.m. for ~16 h, at 16°C, cells were harvested by centrifugation and resuspended in 50 mL lysis buffer (0.3 M NaCl, 50 mM KH₂PO₄, and 10 mM imidazole [pH 8.0]) supplemented with 1 mg/mL lysozyme (Amresco, Solon, OH, USA; 0663) and were incubated on ice for 4 h before being disrupted by sonication on ice. The supernatant was collected after centrifugation at 12,000 rpm at 4°C for 15 min, then 2 mL of a 50% slurry of Ni-NTA Agarose (Qiagen, Hilden, Germany; 30210), equilibrated with lysis buffer, was added to each sample. The mixture was incubated on ice for 30 min with gentle shaking and then placed on an Econo-Pac Chromatography Column (Bio-Rad Laboratories, Hercules, CA, USA; 7321010). Unbound protein was removed by washing the Ni-NTA agarose, three times, with a column volume of wash buffer (0.3 M NaCl, 50 mM KH₂PO₄, and 20 mM imidazole [pH 8.0]), then 2-mL elution buffer (0.3 M NaCl, 50 mM KH₂PO₄, and 250 mM imidazole [pH 8.0]) was applied to elute the His-fusion protein. Next, centrifugal filter devices (Merck Millipore; UFC201024) were used to replace the elution buffer with 1 × Phosphate buffer saline (PBS) buffer (0.14 M NaCl, 2.7 mM KCl, 10 mM Na₂HPO₄, and 1.8 mM KH₂PO₄). Purified protein was quantified using a Pierce BCA Protein Assay Kit (Thermo Fisher Scientific; 23227), then aliquoted, stored at -80°C, and used for the enzyme activity assay. Primers used for vector construction are listed in Supplemental Table 3.

ACS enzyme activity assay

The ACS activity assays were performed, as previously described. This method measures ethylene production, thereby indicating the ACS activity within the tested tissues. The reaction solution, containing 200 mM tricine (pH 8.0), 3.5 μM pyridoxal-L-phosphate, 10 mM dithiothreitol, and 1.2 mM S-(5'-adenosyl)-L-methionine chloride, was freshly prepared. The reaction was initiated by adding 3 μg of purified recombinant enzyme to 1.6 mL reaction solution and incubated for 2 h at 25°C with gentle shaking. The reaction was terminated with 200 μL 100 mM HgCl₂, then 950 μL of the reacted mixture and 850 μL distilled water were combined in a 10-mL glass vial, which was sealed with a cap before

being injected with 0.2 mL NaOH–NaOCl mixture (freshly prepared by mixing two units of 5% NaOCl and one unit of 6 M NaOH on ice). The sample was vortexed for 5 s and placed on ice for 4 min to react, before being vortexed for 5 s again to release the ethylene into the headspace of the glass vial. A 250- μ L aliquot of gas was withdrawn from the headspace, using a syringe, and its ethylene content quantified using an Agilent 6890N gas chromatograph (Agilent Technologies, Santa Clara, CA, USA) fitted with a flame-ionization detector. Results shown are the mean \pm SEM ($n = 3$ replicates).

In situ hybridization assay

Sense and antisense RNA probes were transcribed, *in vitro*, using a digoxigenin RNA labeling kit (Roche, Basel, Switzerland; #11175025910), with the *ACS1*-specific region as a template. Primers used to amplify the template are listed in [Supplemental Table 1](#). Tissue sections were prepared, as previously described (Schneitz *et al.*, 1998), with minor modifications. Briefly, shoot tips were excised and fixed, overnight, in freshly prepared 4% paraformaldehyde at 4°C. Dehydration was performed on ice using an ethanol series from 30% to 100%, for 1 h at each step. The samples in 100% ethanol were then incubated at 37°C for 30 min, infiltrated with Steedman wax, at 37°C for 1 day, and embedded in a small casting mold, before being cut into 20- μ m slices using a microtome (Leica Microsystems, Wetzlar, Germany). Because in our previous *in situ* hybridization experiments, we observed that tissue sections in Steedman wax loosen from the slides, we performed the subsequent steps in RNase-free cell culture dishes. After the slices were stretched in Diethylpyrocarbonate (DEPC)-treated water and the wax was washed with ethanol, tissue sections displaying the complete morphology were selected under a microscope and transferred into cell strainers placed in culture dishes filled with ethanol. Hybridization and staining were performed by transferring the cell strainers through a series of culture dishes filled with the following solutions: 100% ethanol, 5 min; 100% ethanol, 1 min; 95% ethanol, 30 s; 85% ethanol, 30 s; 70% ethanol, 30 s; 50% ethanol, 30 s; 30% ethanol, 30 s; DEPC-treated water, 2 min; PBS, 2 min; proteinase K (10 μ g/mL), 10 min at 37°C; glycine, 2 min; PBS, 2 min, twice; 4% Paraformaldehyde, 10 min; two treatments of PBS for 2 min; hybridization solution at 45°C, overnight; two treatments of 0.2 \times Saline sodium citrate (SSC) at 45°C, 20 min; two treatments of 1 \times Na–Tris–EDTA (NTE) at 37°C, 5 min; RNase A in 1 \times NTE at 37°C, 30 min; two treatments of 1 \times NTE at 37°C, 5 min; 0.2 \times SSC at 45°C, 20 min; 1 \times Tris-buffered saline, 5 min; 1% blocking reagent, 45 min; 1% bovine serum albumin in Tris-buffered saline with Tween-20 (TBST), 45 min; 1:1,000 anti-DIG-antibody at 4°C, overnight; four treatments of TBST with gentle shaking, 15 min; detection buffer (100 mM Tris–HCl, 100 mM NaCl [pH 9.5]), 5 min; Nitroblue tetrazolium chloride/5-bromo-4-chloro-3-indolyl-phosphate (NBT/BCIP) solution, for several hours. When the signal was strong enough, the reaction was terminated using 1 \times TE (Tris–EDTA buffer). The sections

were then transferred onto slides, and images were taken using a digital camera mounted on a Leica DM5500B microscope.

Construction of *ProACS1G:GUS* and *ProACS1f:GUS* fusion genes

For the *ProACS1G:GUS* (β -glucuronidase) reporter construct, DNA fragments covering the upstream 2 kb of the start codon of *ACS1G* were amplified from the genomic DNA of the gynocercous cucumber, CU2-Gy. For the *ProACS1f:GUS* reporter construct, DNA fragments covering the upstream 2 kb of the *ACS1f* start codon were amplified from the genomic DNA of the monoecious cucumber, CU2-Mo. The Sal I and Xba I sites were inserted into the end of the two forward primers and the end of the same reverse primer, respectively. Then, the promoters of *ACS1G* and *ACS1f* were cloned into a binary vector, pCambia1305.4, before the *GUS* coding region. Each fusion construct was confirmed by DNA sequencing. Sequences for the primers are listed in [Supplemental Table 4](#).

Histochemical GUS staining

Histochemical GUS staining of transgenic cucumber floral buds was performed, as previously described (Wang *et al.*, 2014). Shoot tips containing the floral buds were cut, using a scalpel, placed in the GUS staining solution, and then vacuum-infiltrated. After incubation at 37°C for 24 h, the GUS staining was terminated. Chlorophyll was removed by using ethanol and then methanol. Before imaging, tissues were cleared using chloral hydrate. The GUS-positive plant tissues were examined under a bright field microscope (Leica DM5500B, Cambridge, England).

Accession numbers

Sequences from this article can be found in the Cucurbit Genomics Database (www.icugi.org) under accession numbers *CsaV3_6G044400* (*ACS1*), *CsaV3_6G044410* (*MYB1*), *CsaV3_6G044420* (*BCAT*), *CsaV3_1G040170* (*ACS2*), *CsaV3_2G025850* (*ACS11*), *CsaV3_4G024150* (*WIP1*), *CsaV3_6G048630* (*ACO2*), *CsaV3_6G041900* (*ACTIN2*).

Supplemental data

Supplemental Figure 1. Genotype categories of the CRISPR/Cas9-edited *Ff* cucumber plants with dysfunctional *MYB1* or *ACS1/1G*.

Supplemental Figure 2. Sanger sequence analysis of *MYB1* in *MYB1^{fCR}* plants.

Supplemental Figure 3. Sanger sequence analysis of *MYB1* in *MYB1_{All}^{CR}* plants.

Supplemental Figure 4. Sanger sequence analysis of *ACS1* in *ACS1^{fCR}* plants.

Supplemental Figure 5. Sanger sequence analysis of *ACS1/1G* in *ACS1_{All}^{CR}* plants.

Supplemental Figure 6. Genomic verification of the *ACS1G^{H164Y}* (*Ff*) and *ACS1f^{E353K}* (*Ff*) mutants.

Supplemental Figure 7. In gynoeocious lines, *ACS1G* transcripts are dominant in floral buds at the key stage of sex determination.

Supplemental Figure 8. In situ hybridization with sense probes of *ACS1/1G* and *ACO2*.

Supplemental Figure 9. GUS staining pattern in flower buds of *ProACS1G:GUS* and *ProACS1f:GUS* transgenic cucumbers.

Supplemental Figure 10. Flower sex type of *F_wip1* double mutants.

Supplemental Figure 11. Flower sex type of *wip1 acs11* double mutants.

Supplemental Figure 12. Flower sex type of *wip1 aco2* double mutants.

Supplemental Figure 13. Model for the regulation of unisexual flower development in cucumber.

Supplemental Table 1. RNA primers used in this study.

Supplemental Table 2. Genome editing, TILLING, and genotyping primers.

Supplemental Table 3. Protein expression primers.

Supplemental Table 4. Transgenic vector and genomic verification primers.

Supplemental Data Set 1. Data for all statistical analyses performed in this study.

Acknowledgments

We thank Zhizhong Gong (China Agricultural University) for helpful discussion and suggestions for this project.

Funding

This work was supported by the National Key Research and Development Program of China (grant no. 2016YFD0101007), National Natural Science Foundation of China (grant nos. 31530066 to S.H., 31322047 to Z.Z., and 31701933 to J.S.). This work was also supported by the Agricultural Science and Technology Innovation Program of Chinese Academy of Agricultural Science (ASTIP-CAAS and CAAS-XTX2016001), Leading Talents of Guangdong Province Program (grant no. 00201515 to S.H.), the Shenzhen municipal (The Peacock Plan KQTD2016113010482651), Dapeng district governments, Central Public-interest Scientific Institution Basal Research Fund (grant no Y2017PT52), and the “Taishan Scholar” Foundation of the People’s Government of Shandong Province.

Conflict of interest statement. The authors declare no competing interests.

References

- Adams DO, Yang SF (1979) Ethylene biosynthesis: identification of 1-aminocyclopropane-1-carboxylic acid as an intermediate in the conversion of methionine to ethylene. *Proc Natl Acad Sci USA* **76**: 170–174
- Ainsworth C, Buchanan-Wollaston V (1997) Sex determination in plants. *Curr Top Dev Biol* **38**: 167–223
- Aryal R, Ming R (2014) Sex determination in flowering plants: papaya as a model system. *Plant Sci* **217**: 56–62
- Banks JA (2008) MicroRNA, sex determination and floral meristem determinacy in maize. *Genome Biol* **9**: 204
- Boualem A, Troadec C, Camps C, Lemhemi A, Morin H, Sari MA, Fraenkel-Zagouri R, Kovalski I, Dogimont C, Perl-Treves R, et al. (2015) A cucurbit androecy gene reveals how unisexual flowers develop and dioecy emerges. *Science* **350**: 688–691
- Boualem A, Fergany M, Fernandez R, Troadec C, Martin A, Morin H, Sari MA, Collin F, Flowers JM, Pitrat M, et al. (2008) A conserved mutation in an ethylene biosynthesis enzyme leads to andromonoecy in melons. *Science* **321**: 836–838
- Byers RE, Baker LR, Sell HM, Herner RC, Dilley DR (1972) Ethylene: a natural regulator of sex expression of *Cucumis melo* L. *Proc Natl Acad Sci USA* **69**: 717–720
- Chen H, Sun J, Li S, Cui Q, Zhang H, Xin F, Wang H, Lin T, Gao D, Wang S, et al. (2016) An ACC oxidase gene essential for cucumber carpel development. *Mol Plant* **9**: 1315–1327
- Colbert T, Till BJ, Tompa R, Reynolds S, Steine MN, Yeung AT, McCallum CM, Comai L, Henikoff S (2001) High-throughput screening for induced point mutations. *Plant Physiol* **126**: 480–484
- De Martinis D, Mariani C (1999) Silencing gene expression of the ethylene-forming enzyme results in a reversible inhibition of ovule development in transgenic tobacco plants. *Plant Cell* **11**: 1061–1072
- Dellaporta SL, Calderon-Urrea A (1993) Sex determination in flowering plants. *Plant Cell* **5**: 1241–1251
- Galun E (1962) Study of the inheritance of sex expression in the cucumber. The interaction of major genes with modifying genetic and non-genetic factors. *Genetica* **32**: 134–163
- Garcia A, Aguado E, Garrido D, Martinez C, JAMILENA M (2020) Two androecious mutations reveal the crucial role of ethylene receptors in the initiation of female flower development in *Cucurbita pepo*. *Plant J*, doi: 10.1111/tpj.14846
- Gu HT, Wang DH, Li X, He CX, Xu ZH, Bai SN (2011) Characterization of an ethylene-inducible, calcium-dependent nuclease that is differentially expressed in cucumber flower development. *New Phytol* **192**: 590–600
- Hao YJ, Wang DH, Peng YB, Bai SL, Xu LY, Li YQ, Xu ZH, Bai SN (2003) DNA damage in the early primordial anther is closely correlated with stamen arrest in the female flower of cucumber (*Cucumis sativus* L.). *Planta* **217**: 888–895
- Hu B, Li D, Liu X, Qi J, Gao D, Zhao S, Huang S, Sun J, Yang L (2017) Engineering non-transgenic gynoeocious cucumber using an improved transformation protocol and optimized CRISPR/Cas9 system. *Mol Plant* **10**: 1575–1578
- Iwahori S, Lyons JM, Smith OE (1970) Sex expression in cucumber plants as affected by 2-chloroethylphosphonic acid, ethylene, and growth regulators. *Plant Physiol* **46**: 412–415
- Knopf RR, Trebitsh T (2006) The female-specific *Cs-ACS1G* gene of cucumber. A case of gene duplication and recombination between the non-sex-specific 1-aminocyclopropane-1-carboxylate synthase gene and a branched-chain amino acid transaminase gene. *Plant Cell Physiol* **47**: 1217–1228
- Kubicki B (1969a) Investigations on sex determination in cucumber (*Cucumis sativus* L.). V. Genes controlling intensity of femaleness. *Genet Pol* **10**: 69–85
- Kubicki B (1969b) Investigations of sex determination in cucumber (*Cucumis sativus* L.). VI. Androecism *Genet Pol* **10**: 87–99
- Kubicki B (1969c) Investigations on sex determination in cucumber (*Cucumis sativus* L.). VII. Andromonoecism and hermaphroditism. *Genet Pol* **10**: 101–120
- Li Z, Huang S, Liu S, Pan J, Zhang Z, Tao Q, Shi Q, Jia Z, Zhang W, Chen H, et al. (2009) Molecular isolation of the M gene suggests that a conserved-residue conversion induces the formation of bisexual flowers in cucumber plants. *Genetics* **182**: 1381–1385
- Ma WJ, Pannell JR (2016) Sex determination: separate sexes are a double turnoff in melons. *Curr Biol* **26**: R171–R173

- Malepszy S, Niemirowicz-szczytt K** (1991) Sex determination in cucumber (*Cucumis sativus*) as a model system for molecular-biology. *Plant Sci* **80**: 39–47
- Martin A, Troadec C, Boualem A, Rajab M, Fernandez R, Morin H, Pitrat M, Dogimont C, Bendahmane A** (2009) A transposon-induced epigenetic change leads to sex determination in melon. *Nature* **461**: 1135–1138
- Mibus H, Tatlioglu T** (2004) Molecular characterization and isolation of the *Fff* gene for femaleness in cucumber (*Cucumis sativus* L.). *Theor Appl Genet* **109**: 1669–1676
- Neff MM, Neff JD, Chory J, Pepper AE** (1998) dCAPS, a simple technique for the genetic analysis of single nucleotide polymorphisms: experimental applications in *Arabidopsis thaliana* genetics. *Plant J* **14**: 387–392
- Perl-Treves R** (1999) Male to female conversion along the cucumber shoot: approaches to studying sex genes and floral development in *Cucumis sativus*. *Sex Determination Plants* 189–215
- Saito S, Fujii N, Miyazawa Y, Yamasaki S, Matsuura S, Mizusawa H, Fujita Y, Takahashi H** (2007) Correlation between development of female flower buds and expression of the *CS-ACS2* gene in cucumber plants. *J Exp Bot* **58**: 2897–2907
- Schmittgen TD, Livak KJ** (2008) Analyzing real-time PCR data by the comparative C(T) method. *Nat Protoc* **3**: 1101–1108
- Schneitz K, Baker SC, Gasser CS, Redweik A** (1998) Pattern formation and growth during floral organogenesis: *HUELLENLOS* and *AINTEGUMENTA* are required for the formation of the proximal region of the ovule primordium in *Arabidopsis thaliana*. *Development* **125**: 2555–2563
- Shiber A, Gaur R, Rimon-Knopf R, Zelcer A, Trebitsh T, Pitrat M** (2008) The origin and mode of function of the Female locus in cucumber. Proceedings of the IXth EUCARPIA meeting on genetics and breeding of Cucurbitaceae (Pitrat M, ed), INRA, Avignon, May 21–24th, 2008.
- Sun JJ, Li F, Li X, Liu XC, Rao GY, Luo JC, Wang DH, Xu ZH, Bai SN** (2010) Why is ethylene involved in selective promotion of female flower development in cucumber? *Plant Signal & Behav* **1052–1056**
- Sun JJ, Li F, Wang DH, Liu XF, Li X, Liu N, Gu HT, Zou C, Luo JC, He CX, et al.** (2016) CsAP3: a Cucumber homolog to *Arabidopsis* APETALA3 with novel characteristics. *Front Plant Sci* **7**: 1181
- Tadmor Y, Katzir N, Meir A, Yaniv-Yaakov A, Sa'ar U, Baumkoler F, Lavee T, Lewinsohn E, Schaffer A, Burger J** (2007) Induced mutagenesis to augment the natural genetic variability of melon (*Cucumis melo* L.). *Israel J Plant Sci* **55**: 159–169
- Tanurdzic M, Banks JA** (2004) Sex-determining mechanisms in land plants. *Plant Cell* **16 (Suppl)**: S61–71
- Trebitsh T, Staub JE, O'Neill SD** (1997) Identification of a 1-amino-cyclopropane-1-carboxylic acid synthase gene linked to the female (*F*) locus that enhances female sex expression in cucumber. *Plant Physiol* **113**: 987–995
- Wang DH, Li F, Duan QH, Han T, Xu ZH, Bai SN** (2010) Ethylene perception is involved in female cucumber flower development. *Plant J* **61**: 862–872
- Wang H, Sui X, Guo J, Wang Z, Cheng J, Ma S, Li X, Zhang Z** (2014) Antisense suppression of cucumber (*Cucumis sativus* L.) sucrose synthase 3 (*CsSUS3*) reduces hypoxic stress tolerance. *Plant Cell Environ* **37**: 795–810
- Wittwer SH, Hillyer IG** (1954) Chemical induction of male sterility in Cucurbits. *Science* **120**: 893–894
- Xing HL, Dong L, Wang ZP, Zhang HY, Han CY, Liu B, Wang XC, Chen QJ** (2014) A CRISPR/Cas9 toolkit for multiplex genome editing in plants. *BMC Plant Biol* **14**: 327
- Yamasaki S, Fujii N, Matsuura S, Mizusawa H, Takahashi H** (2001) The *M* locus and ethylene-controlled sex determination in andromonoecious cucumber plants. *Plant Cell Physiol* **42**: 608–619
- Yin T, Quinn JA** (1992) A mechanistic model of a single hormone regulation both sexes in flowering plants. *Bull Torrey Bot Club* **119**: 431–441
- Zhang J, Guo S, Ji G, Zhao H, Sun H, Ren Y, Tian S, Li M, Gong G, Zhang H, et al.** (2020) A unique chromosome translocation disrupting *CIWIP1* leads to gynoecey in watermelon. *Plant J* **101**: 265–277
- Zhang Z, Mao L, Chen H, Bu F, Li G, Sun J, Li S, Sun H, Jiao C, Blakely R, et al.** (2015) Genome-wide mapping of structural variations reveals a copy number variant that determines reproductive morphology in cucumber. *Plant Cell* **27**: 1595–1604